DOI: 10.24996/ijs.2024.65.5.45

ISSN: 0067-2904

Determining The Agricultural Drought and Desertification Intensity in Diyala Province / Iraq Using Sentinel-2 images

Rana S. Hadid, Bushra A. Ahmed*

University of Baghdad, College of Science, Remote Sensing and GIS Department

Received: 2/3/2023 Accepted: 15/5/2023 Published: 30/5/2024

Abstract

Desertification is the deterioration of land brought on by human activity, climate change, and a loss of vegetation cover and biodiversity. This paper assesses the agricultural drought and desertification levels of Khanaqin district in Diyala province, Iraq, using Sentinel-2 images with a high resolution of 10 m between July 22, 2016, and July 22, 2022. The Modified Soil-Adjusted Vegetation Index (MSAVI2), Topsoil Grain Size Index (TGSI), and Salinity Index (SI) derived from Sentinel-2 satellite images were used for this aim. The result showed that the area covered by low desertification intensity increased from (12.05%-9.41%) for the years (2016-2022). The area covered by high desertification intensity increased from (32.49-36.44% for the years (2016-2022), indicating an accelerated desertification process. Finally, the area covered by high desertification intensity increased from 12.34%-21.23% for years (2016-2022). Natural climate variability and human activities, such as land use, overgrazing, deforestation, and unsustainable farming practices, cause agricultural drought and desertification.

Keywords: Sentinel-2; Spectral Indices; Desertification; MSAVI2; SI; TGSI.

تحديد شدة الجفاف الزراعي والتصحر في محافظة ديالى / العراق باستخدام صور Sentinel-2

رنا حديد ، بشرى علي احمد*

وحدة الاستشعار عن بعد، كلية العلوم، جامعة بغداد، بغداد، العراق

الخلاصة

التصحر هو تدهور الأراضي الناجم عن النشاط البشري وتغير المناخ وفقدان غطاء النباتات والتنوع الحيوي. تم دراسة منطقة خانقين في محافظة ديالى بالعراق باستخدام صور الأقمار الصناعية من نوع Sentinel-2 بدقة عالية 10 أمتار بين 22 تموز 2016 و22 تموز 2022. لتقييم مستويات الجفاف الزراعي والتصحر في منطقة الدراسة، تم استخدام عدد من المؤشرات الخاصة بالنبات والتربة مثل Modified Soil-Adjusted Vegetation Index (MSAVI2) ، و Topsoil Grain Size Index (TGSI)، و Salinity Index (SI) المستمدة من صور الأقمار الصناعية Sentinel-2. أظهرت النتائج زيادة المساحة التي تغطيها شدة التصحر المنخفضة من 12.05٪ في عام 2016 إلى 9.41٪ في عام 2022. زادت المساحة التي تغطيها شدة التصحر العالية من 32.49٪ في عام 2016 إلى 36.44٪ في عام 2022، مما يدل على تسارع عملية التصحر. وأخيرًا، زادت المساحة التي تغطيها شدة التصحر الشديد جدًا من 12.34٪ في عام 2016 إلى 21.23٪ في عام 2022. ومن أسباب الجفاف الزراعي والتصحر هو التغيرات المناخية

*Email: bushra.a@sc.uobaghdad.edu.iq

الطبيعية والأنشطة البشرية مثل استخدام الأراضي والرعي المفرط وإزالة الغابات وممارسات الزراعة غير المستدامة.

1. Introduction

Desertification is a term used to describe the degradation of land brought on by human activity and climate change in arid, semi-arid, and dry sub-humid regions[1]. The phenomenon of desertification is among the most important contemporary environmental problems, as the continued depletion of vegetation cover leads to an increase in the deterioration of agricultural lands and their productivity. It is necessary to distinguish between desiccation (long-term drought) and desertification. The term drought is used to refer to an inter-annual fluctuation in precipitation in which there is a relative lack of rainfall for a period of one to four years, whereas desertification is used to denote a protracted drought that has continued for a decade or more and may be considered a kind of climate change[2]. Drought reduces the number and condition of vegetation and soil cover and thus increases soil erosion. Desertification has a much more profound impact, and deserted soils are highly susceptible to wind and erosion and thus lose a large part of their depth and capacity to store water and nutrients[3].

Iraq is experiencing a water shortage due to low rainfall, ineffective water resources management, and decreased water flow into the Tigris and Euphrates rivers from upstream nations[4]. Due to these conditions, some phenomena are born, including desertification. Together, these factors have resulted in a decline in the quality and volume of natural vegetation in Iraq, the removal of topsoil, and a decline in the productivity of the land and food production[5].

Remote sensing has shown to be a reliable method of identifying soil changes, natural flora, land usage, and desertification. Using satellite imagery is highly effective for observing alterations to the earth's surface and its coverage[6]. Satellite data multi-temporal coverage[7] uses pictures to track changes in land use and coverage over time, which can be used to fight desertification and lessen its effects in arid and semiarid regions[8]. Vegetation is one of the most critical facets for decreasing drought impacts and determining the severity of desertification[9]. Many agricultural drought and desertification intensity monitoring methods have been proposed and developed. Data and indices obtained from various sensors or satellites, such as the Sentinel-2 imagers, also showed a significant impact. High-resolution Sentinel-2 images are accessible through the Copernicus program (10 m). Sentinel-2 imageries are used to monitor crop health, area, and productivity for regular and irregular farms due to their high spatial resolution compared to Landsat satellites, which are anticipated to produce more accurate data [10].

Based on correlation analysis between the new spectral and statistical ranges and using the spectral indices' methodology for water, soil, and vegetation cover, the desertification degrees and agricultural drought were determined using MSAVI2, TGSI, and SI.

1.2. Previous studies

Several previous studies have been conducted on determining agricultural drought and desertification intensity in Iraq using satellite images. Y. K. Al-timimi (2012) used remote sensing and GIS techniques to investigate drought levels in Iraq. Meteorological and Agricultural droughts were calculated based on (SPI (Standardized Precipitation Index) and NDVI. The study prepared drought risk maps by calculating the frequency of droughts and integrating agriculture and meteorological drought risk maps. The study found that 14.4% of the area has Slight drought, 61.6% faces moderate risk, 23.2% suffers from a severe risk, and 0.8% suffers from a severe risk, with northwest Iraq being more drought-prone [11]. F. A. Zwain (2021) utilized remote sensing data and image analysis tools to detect and monitor desertification in Basra province. The study evaluated the potential of remote sensing analysis in desertification monitoring using three Landsat images captured in 1973, 1993, and 2013. The results showed significant environmental changes in the arid zone of Basra province, such as declining surface water, degradation of agricultural lands, and deterioration of marshlands [12]. B. Abdulrahman (2018) mentioned that remote sensing techniques, including supervised classification, have been used to monitor and classify the land cover for the Al-Shari Lake region. The results showed that high-density arable land and permanently irrigated areas increased slightly from 13.0% to 13.3% between 1996 and 2017. Low-density arable land intermixed with fallow land decreased from 54.5% to 51.6%, and dunes and rocks remained relatively stable at 7.7%. Abandoned land and saline decreased from 2.0% to 1.8%, and water bodies in winter decreased from 1.9% to 0.9% between 1996 and 2017 [13]. H. S. Abbas (2019) focused on the desertification problem and vegetation cover degradation in Al-Muthana, a semi-arid area in southern Iraq. The researchers used Ladsat-8 images with a 15m spatial resolution to collect ground truth data, including rainfall, temperature, digital elevation model (DEM), and soil texture characteristics. The extracted data could be presented in tables, figures, and GIS maps to represent the distribution of various factors affecting desertification in the region [14]. Allawi, M. F. (2020) used GIS and remote sensing techniques to assess changes in land cover within Mosul Province, Iraq, between 2014 and 2018, using Landsat 8 satellite images and normalized difference vegetation index (NDVI). Results showed a fluctuation in vegetative distribution, with a ratio of 4.98% in 2014, decreasing to 4.77% in 2015 and 3.54% in 2016, then increasing to 4.39% in 2018. The highest NDVI value was found in 2015, indicating moderate to high vegetation cover[15]. This study aims to use remote sensing techniques to assess agricultural drought and desertification, identify changes in land cover, recognize deterioration, and determine the impact of sand encroachment in the

2. Material and methods

2.1. Study Area

Khanaqin district, with its three sub-districts (Khanaqin center, Jalawla, and Al-Saadiya), occupies the northeastern part of Diyala Province and is confined between longitudes (45° 21' 10"-45° 30' 30") E and latitudes (34° 15' 11"-34° 22' 00”) N[16]. Its administrative borders are bordered by Sulaymaniyah province from the north, Iran from the east, Baladruz and Al-Muqdadiya districts from the south, and Kafri and Al-Khalis districts from the west, Figure (1).

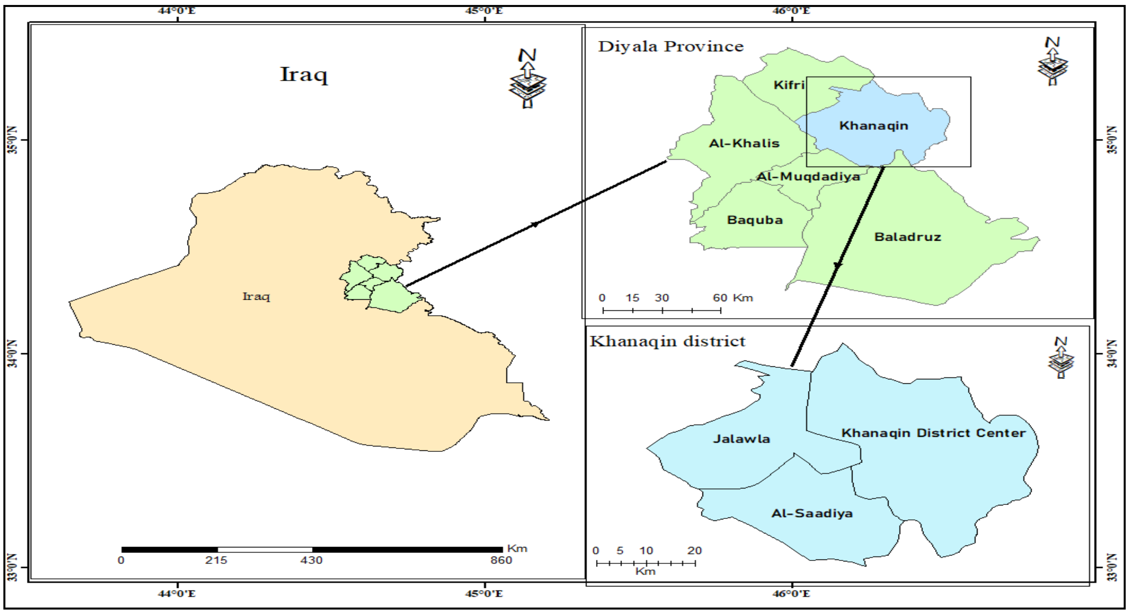

Figure 1: Map of the study area, Khanaqin.

2.2. Sentinel-2 data and pre-processing

The Diyala province agricultural drought and desertification intensity were mapped using a Sentinel-2 (S2) satellite. The Sentinel-2 satellite image (Level-1C) was downloaded for free from the Copernicus Open Access Hub (https://scihub.copernicus.eu). Two identical satellites, Sentinel-2A, and Sentinel-2B, are part of the sentinel-2 mission. Sentinel-2A and Sentinel-2B were available in November 2015 and March 2017, respectively. The spatial resolution of Sentinel-2 images ranges from 10 to 60 m[17].

The image was captured during two separate periods: February 14, 2016, February 27, 2022, July 22, 2016, and July 22, 2022. Various product levels are accessible to users, but this study specifically used Level-2A, which provides bottom-of-atmosphere (BOA) reflectance. To achieve this format, the S2 L1C data underwent preemptive conversion through the Sen2Cor algorithm accessible through the free SNAP software provided by the European Union's ESA.[18]. The pre-processing also included resampling bands to 10m spatial resolution using the nearest neighbor algorithm in SNAP software, extraction, and clipping the study site from the scene. The analysis utilized Band 2 (Blue), Band 3 (Green), Band 4 (Red), and Band 8 (NIR) with a 10 m resolution (Table 1)[19].

The reason for selecting a cloudless scene during summertime is when crops typically had harvested, and the density of natural and annual flora is at its lowest. This period is considered optimal for measuring desertification in the research region since it helps avoid confusion between desertification and seasonal vegetation.

Table 1: Bands properties for Sentinel-2, wavelength and resolution.

Sentinel-2 Bands	***Central Wavelength (μm)***	***Resolution (m)***
Band 2 - Blue	0.490	10
Band 3 - Green	0.560	10
Band 4 - Red	0.665	10
Band 8 - NIR	0.842	10

2.3. Spectral indicator analysis

The desertification process can be seen most clearly in the vegetation's greenness or biomass alteration; indices can measure desertification that considers these changes [20]. Several spectral indices were employed in this study, including:

2.3.1.The Modified Soil-Adjusted Vegetation Index (MSAVI2):

The MSAVI2 aims to resolve some NDVI limitations when used in areas where the soil surface is highly exposed [21]. The MSAVI2 approach is less sensitive to bare soil than the SAVI [22]. MSAVI2 values range from $^-1$ to $^+1$, with $^-1$ and 0 denoting non-plant characteristics, including barren ground, a built-up region, and a water body, while the value of $^+1$ and larger indicating vegetation cover [23][18], as shown in Eq. (1) [22].

$$\text{MSAVI2} = 2 * NIR + 1 - \frac{\sqrt{(2 * NIR + 1)^2 - 8 * (NIR - RED)}}{2} \quad (1)$$

2.3.2. Topsoil Grain Size Index (TGSI):

TGSI was utilized to determine the topsoil layer's grain size composition or surface soil texture. TGSI was utilized to monitor desertification in dry areas [24]. Red, blue, and green bands from the Sentinel-2 image were used to determine the TGSI, Eq. (2). The range of TGSI values was inversely associated with the amount of fine sand from 1 to $^+1$. Positive numbers or those close to 0 represent areas with flora or water bodies, while values close to 0.20 signify large concentrations of fine sand [25].

$$\mathrm{TGSI} = \frac{B4-B2}{B4+B3+B4} \quad (2)$$

2.3.3 Salinity Index (SI):

Soil salinization is a major land degradation process in arid and semi-arid regions characterized by high temperatures and low precipitations [12]. Salinization is a land degradation that negatively affects soil quality and plant growth, leading to land desertification [26]. The SI index uses green and red bands, as shown in Eq.(3), using Sentinel-2 Band 3 (Green) and Band 4 (Red) [27].

$$\mathrm{Sentinel} - 2\ \mathrm{SI} = \mathrm{Index}(\mathrm{B3}, \mathrm{B4}) = \frac{B3+B4}{2} \quad (3)$$

4. RESULTS AND DISCUSSION

Based on the analysis of Sentinel-2 images using various spectral indicators, it can be concluded that Diyala Province is experiencing moderate to severe levels of agricultural drought and desertification. The GSI, MSAVI2, and SI were used to assess the intensity of drought and desertification.

4.1. MSAVI2 vegetative index results

The area had the highest percentage of low vegetation density in February 2016 at 36.2%, followed by barren land at 21.8%, water at 10.3%, medium vegetation density at 18.5%, good vegetation density at 8.8%, and high vegetation density at 4.3%. In July 2016, there was a decrease in the proportion of low vegetation density to 24.48%, while barren land increased significantly to 57.88%. On February 27, 2022, the proportion of low vegetation density had further decreased to 19.44%, while barre+n land decreased slightly to 66.48%. On July 22, 2022, the proportion of low vegetation density decreased to 13.61%, while barren land increased again to 78.38%.

Overall, the area has been subjected to a decrease in low vegetation density and increased barren land over time. Water has also decreased, while medium, good, and high vegetation densities have fluctuated.

Table 2: MSAVI2 vegetative index between February 14, 2016, and February 27, 2022

MSAVI2 for years	Vegetation density	Area (Km^2)	The ratio (%)
2016	low vegetation density	920.2865	36.2
	medium vegetation density	470.549	18.5
	good vegetation density	223.6476	8.8
	high vegetation dense	110.2692	4.3
	water	262.9354	10.3
	barren land	553.6812	21.8
2022	low vegetation density	493.9199	19.44
	medium vegetation density	132.8949	5.23
	good vegetation density	104.7277	4.12
	high vegetation dense	59.5783	2.34
	water	60.8204	2.39
	barren land	1689.4233	66.48

Table 3: MSAVI2 vegetative index between July 22, 2016, and July 22, 2022

MSAVI2 for years	Vegetation density	Area (Km^2)	The ratio (%)
2016	low vegetation density	622.2322	24.48
	medium vegetation density	94.7853	3.73
	good vegetation density	45.5629	1.79
	high vegetation dense	27.1851	1.07
	water	280.7695	11.05
	barren land	1470.8247	57.88
2022	low vegetation density	345.8138	13.61
	medium vegetation density	87.29	3.43
	good vegetation density	46.0461	1.81
	high vegetation dense	25.1058	0.99
	water	45.1457	1.78
	barren land	199.19625	78.38

Source: Sentinel-2A (L2A) MSI satellite image analysis, 10-m resolution, July 22, 2016, and July 22, 2022, using Arc GIS Pro3.0.2 program.

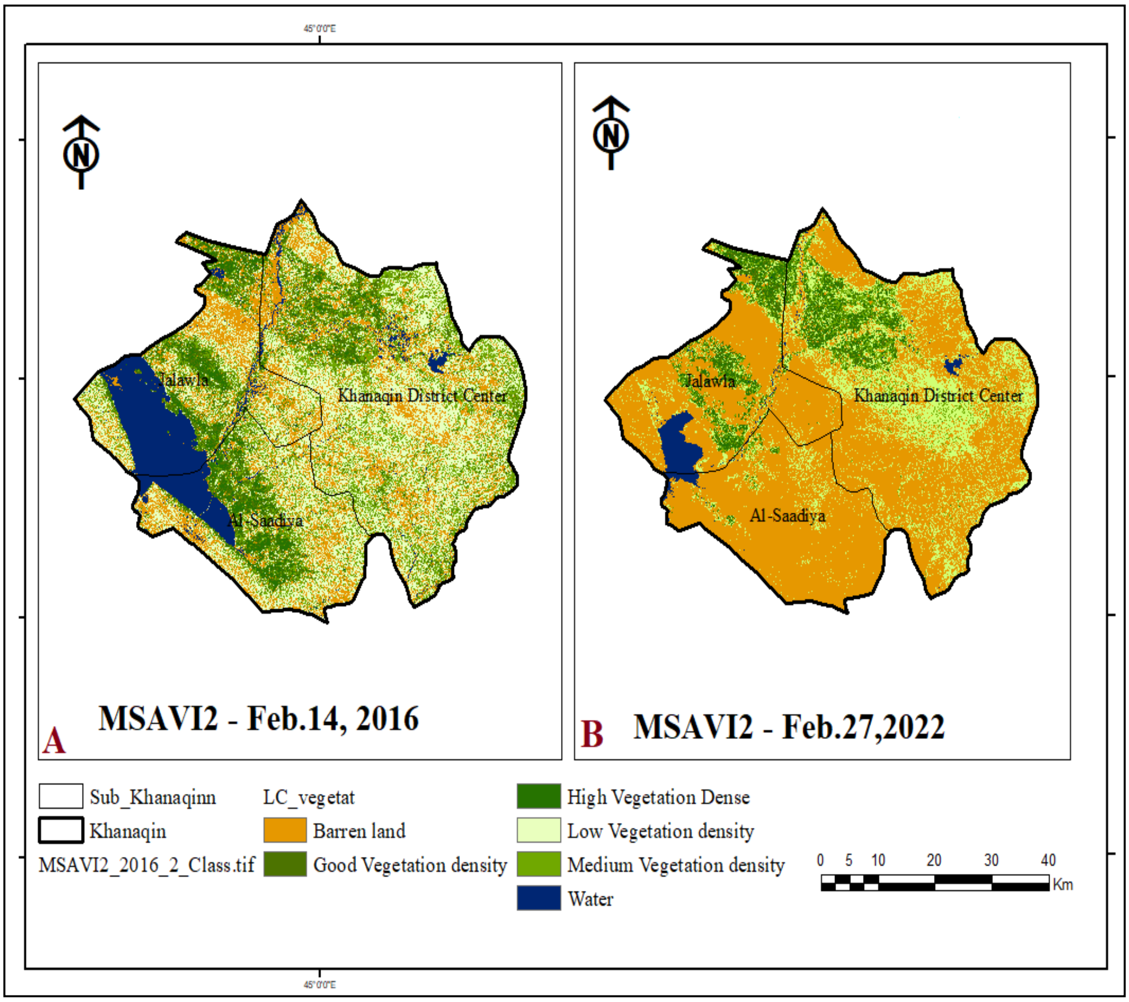

Figure 2: MSAVI2 for the study area between February 14, 2016, and February 27, 2022

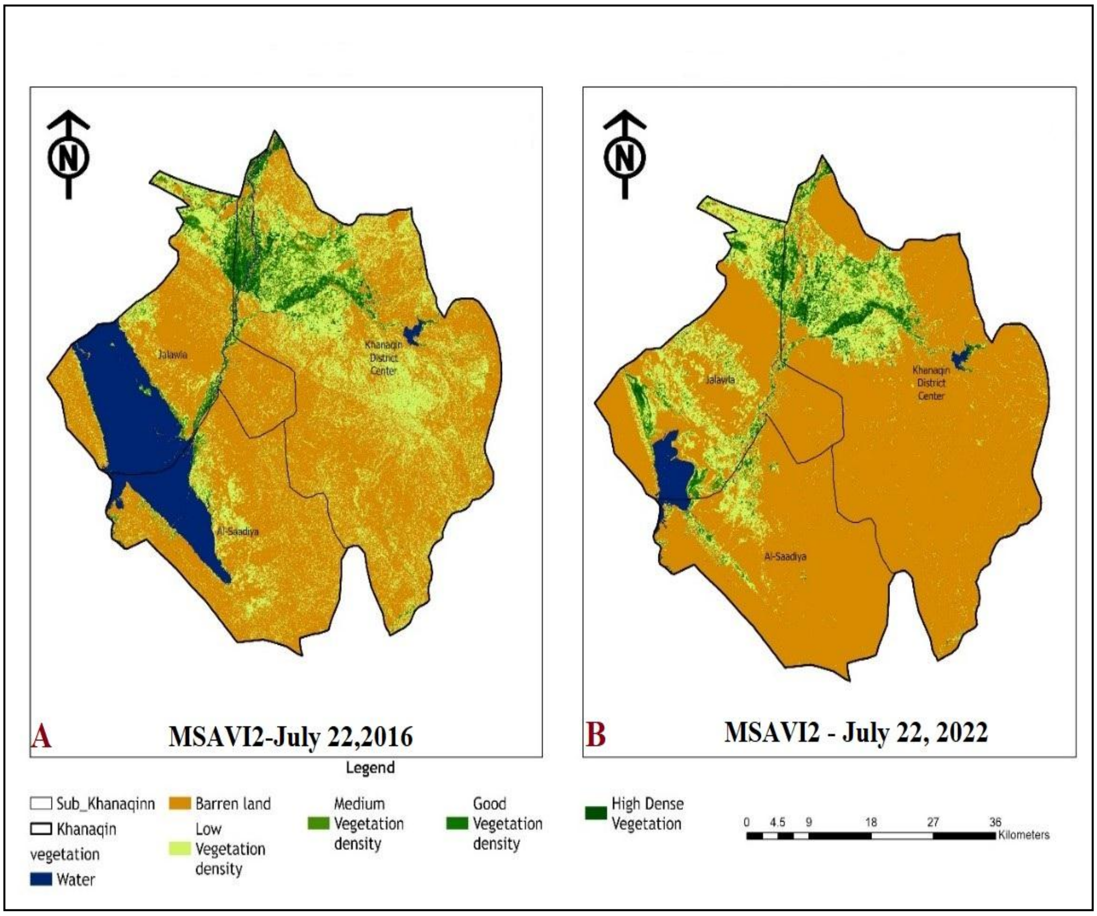

Figure 3: MSAVI2 for the study area during (A): July 22, 2016, (B) MSAVI2 July 22, 2022.

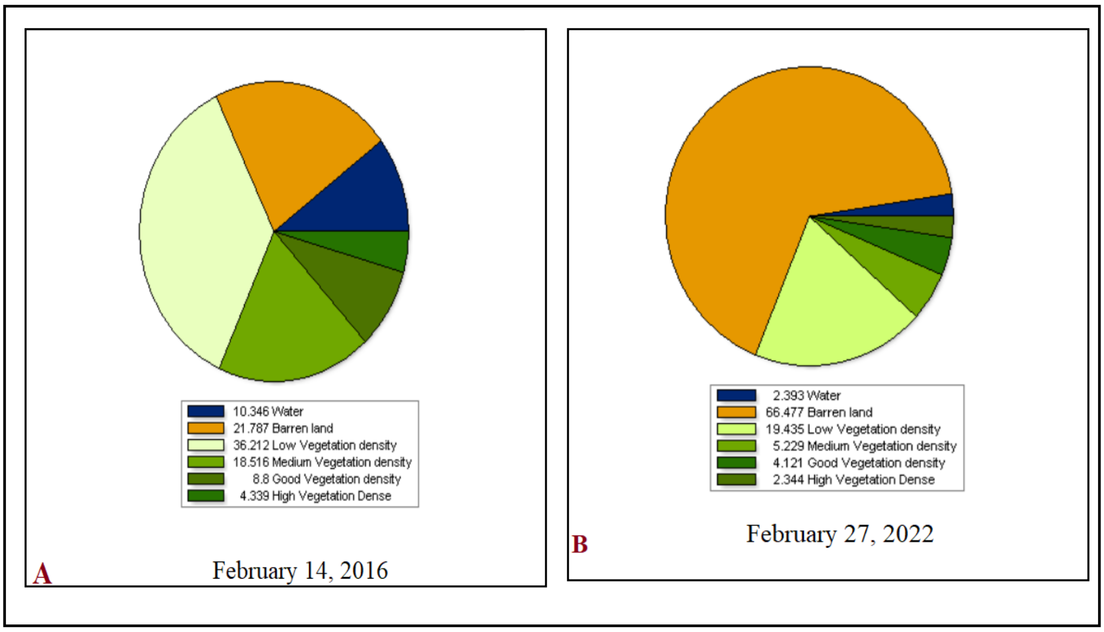

Figure 4: Pie chart of MSAVI2 during (A): February 14, 2016, (B) February 27, 2022

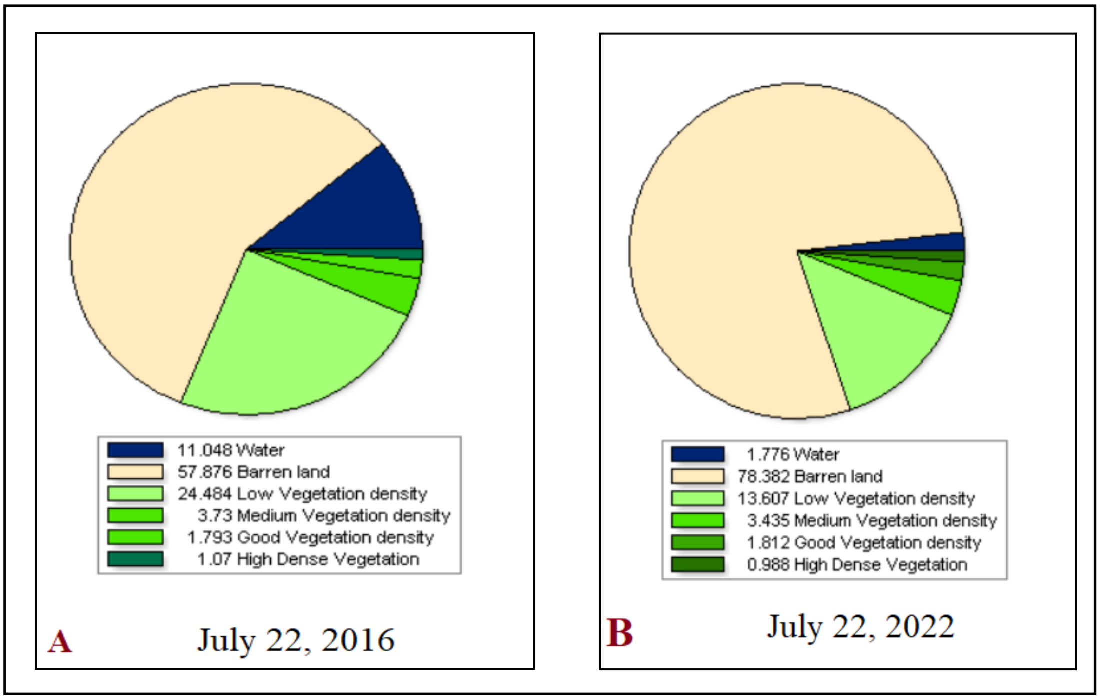

Figure 5: Pie chart of MSAVI2 classes during: (A) July 22, 2016, and (B) July 22, 2022.

4.2. Results of the Topsoil grain size index (TGSI)

The results show that there has been a significant decrease in the percentage of land covered by vegetation and an increase in the percentage of land covered by desert between 2016 and 2022. The percentage of land covered by water bodies has decreased slightly, while the percentage of land covered by medium and high contents of fine sand has remained relatively unchanged., Figure 6 and Table 4.

These changes in land cover can significantly impact the ecosystem and environment, such as water availability, biodiversity, and climate. Monitoring and understanding these changes is essential to develop appropriate sustainable land use and management strategies.

Table 4: TGSI of the land cover between July 22, 2016, and July 22, 2022

TGSI for years	Landcover by TGSI	Area (Km^2)	The ratio (%)
2016	soil covered by water bodies	25.17837	10
	soil covered by vegetation	10.27009	4
	medium contents of fine sand	51.9912	20
	high contents of fine sand	114.46521	45
	soil is fully covered by fine sand (desert)	52.2311	21
2022	soil covered by water bodies	5.04754	2
	soil covered by vegetation	10.57772	4
	medium contents of fine sand	47.40679	19
	high contents of fine sand	104.11983	41
	soil is fully covered by fine sand (desert)	86.93792	34

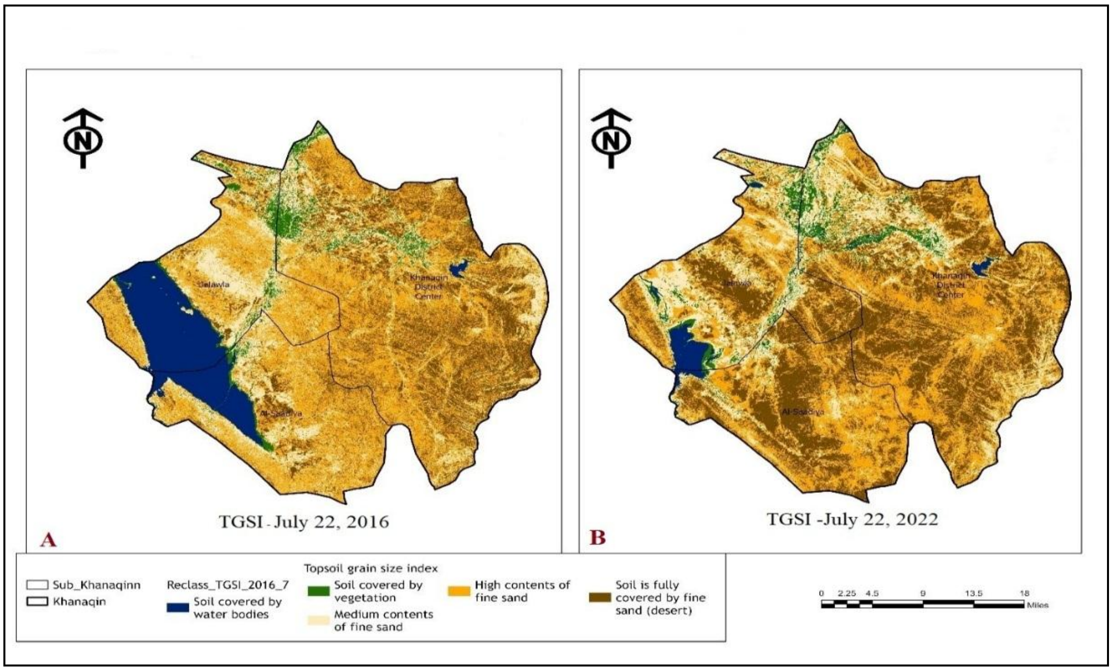

Figure 6: Spatial variation of soil surface texture in Khanaqin district between 2016 and 2022

4.3. Results of the Salinity Index (SI):

Between 2016 and 2022, there have been significant changes in the salinity index and corresponding desertification intensity types. The area covered by low salinity and no desertification decreased from 12.11% to 5.06%, indicating an increase in soil salinity and desertification. The area transitioning from low to moderate desertification increased from 12.05% to 9.41%. The desertification rate slowed down for the area with high salinity and moderate desertification intensity, which increased from 31.01% to 27.86%. However, a very high salinity area and high desertification intensity increased from 32.49% to 36.44%, and the area with extremely high salinity and very high desertification intensity increased from 12.34% to 21.23%. These results indicate an accelerated desertification process and the need for urgent measures to mitigate the process, Figure 7, Figure 8, and Table 5.

Table 5: salinity and desertification intensity between 2016 and 2022.

Salinity Index for years	Landcover by Salinity Index	Area (km^2)	The ratio (%)
2016	low salinity and no desertification	307.8292	12.11
	moderate salinity and low desertification intensity	306.1644	12.05
	high salinity and moderate desertification intensity	788.0455	31.01
	very high salinity and high desertification intensity	825.7476	32.49
	extremely high salinity and very high desertification intensity	313.573	12.34
2022	low salinity and no desertification intensity	128.631	5.06
	moderate salinity and low desertification intensity	239.094	9.41
	high salinity and moderate desertification intensity	708.1435	27.86
	very high salinity and high desertification intensity	925.9806	36.44
	extremely high salinity and very high desertification intensity	539.5148	21.23

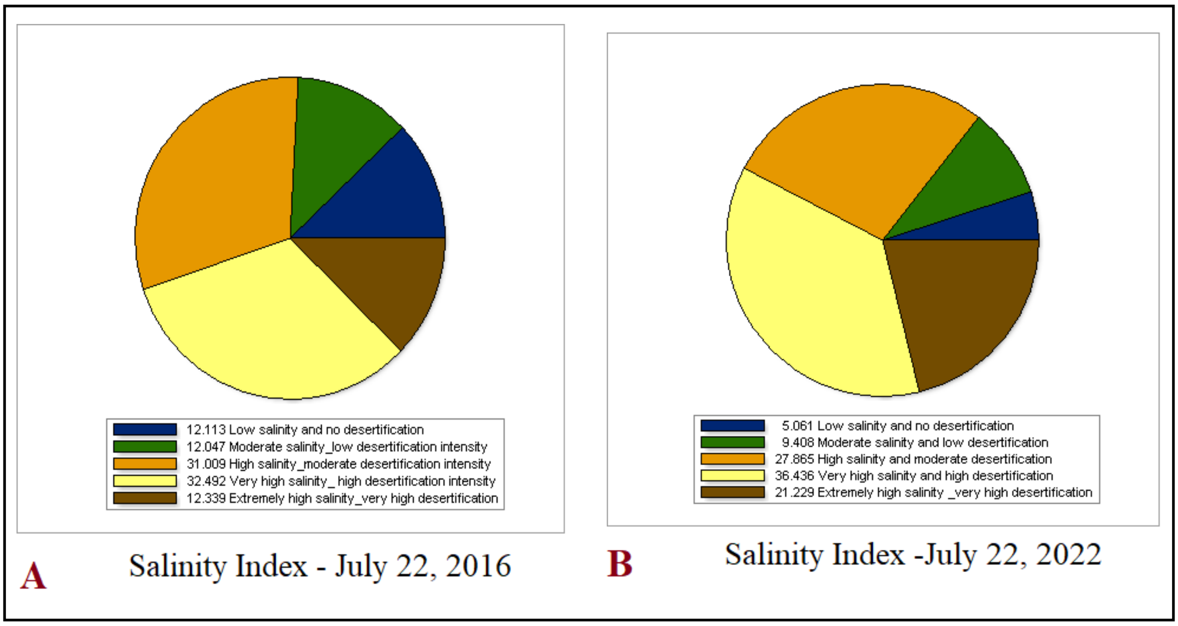

Figure7: Pie chart of Salinity Index classes for July 22, 2016, and July 22, 2022.

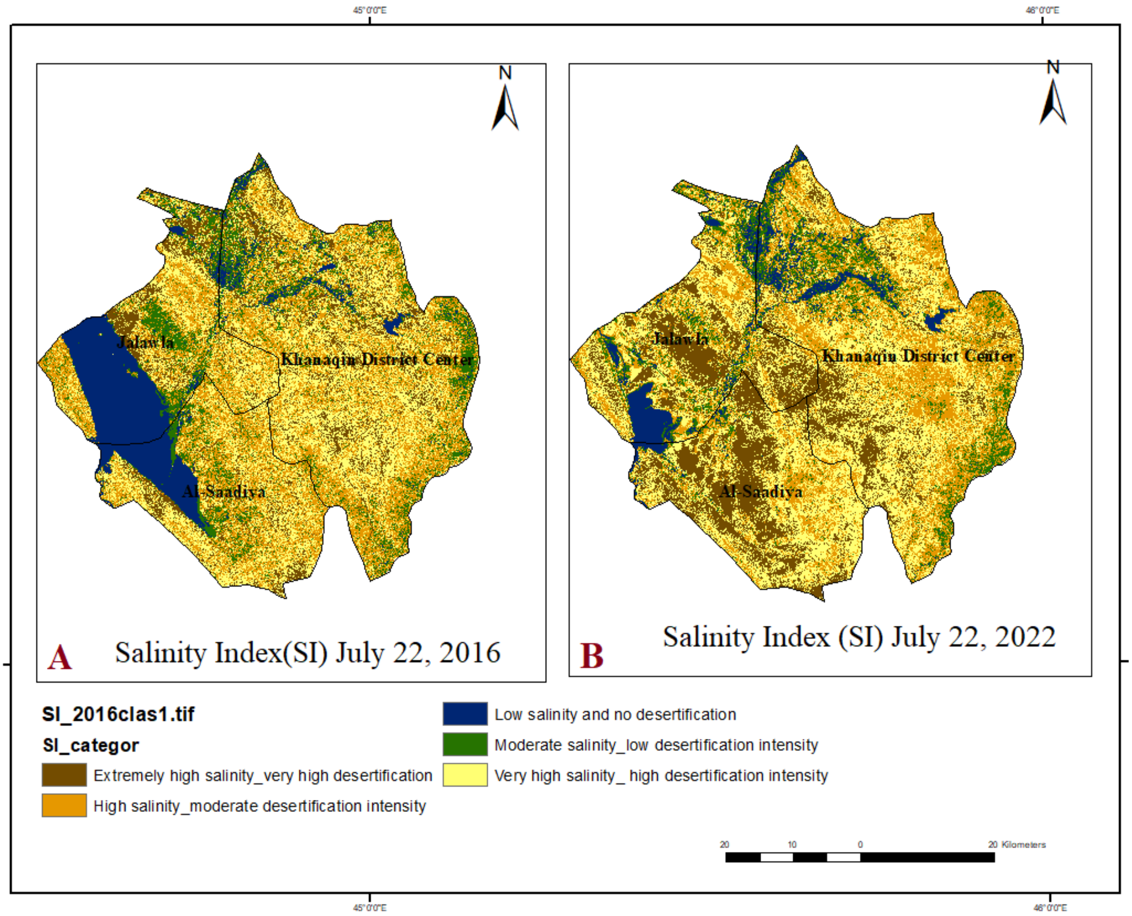

Figure 8: salinity and desertification intensity in Khanaqin district between 2016 and 2022.

5. Conclusions and Recommendations

The study analyzed Sentinel-2 images and various spectral indicators to determine the intensity of agricultural drought and desertification in Diyala Province, Iraq. The results showed that the province is facing moderate to severe levels of drought and desertification, with high levels of vegetation stress and water shortage. The Topsoil Grain Size (GSI), Modified Soil-Adjusted Vegetation Index 2 (MSAVI2), and Salinity Index (SI): were used to assess the intensity of drought and desertification.

To mitigate the impact of agricultural drought and desertification, the study recommends implementing efficient water management techniques such as rainwater harvesting and drip irrigation, soil conservation practices such as contour farming and conservation tillage, crop diversification by introducing drought-tolerant crops, and reforestation programs. Implementing these measures can minimize the impact of drought and desertification, and the region's agricultural productivity can be improved.

References

[1] A. A. Lamqadem, B. Pradhan, H. Saber, and A. Rahimi, "Desertification sensitivity analysis using medalus model and gis: A case study of the oases of middle Draa valley, morocco," *Sensors (Switzerland),* vol. 18, no. 7. 2018. doi: 10.3390/s18072230.

[2] A. A. Jasim, "Monitoring Desertification in Badra Area Eastern Iraq by Using Landsat Image Data." 2012.

[3] V. R. Squires, "Desertification and Drought," *Handb. Drought Water Scarcity*, pp. 13–26, Aug. 2017, doi: 10.1201/9781315404219-2.

[4] "Iraq: Droughts - DREF Operation n° MDRIQ013 - Operation update n° 1 - Iraq | ReliefWeb." https://reliefweb.int/report/iraq/iraq-droughts-dref-operation-ndeg-mdriq013-operation-update-ndeg-1 (accessed Mar. 14, 2023).

[5] E. T. Al-khaqani, "Desertification Detection by NDVI and Other Indices: A Case Study in Najaf," *J. Xidian Univ.*, vol. 14, no. 9, 2020, doi: 10.37896/jxu14.9/126.

[6] M. Allawai, B. A.-I. C. S. Materials, and undefined 2020, "Using remote sensing and GIS in measuring vegetation cover change from satellite imagery in Mosul City, North of Iraq," *iopscience.iop.org*, doi: 10.1088/1757-899X/757/1/012062.

[7] C. K. Musyoka, "Monitring Desertification Using Remote Sensing for Environmental Management; A Case Study of Kitui County," *Angewandte Chemie International Edition, 6(11), 951–952.* pp. 10–27, 2021.

[8] A. A. Lamqadem, H. Saber, and B. Pradhan, "Quantitative Assessment of Desertification in an Arid Oasis Using Remote Quantitative Assessment of Desertification in an Arid Oasis Using Remote Sensing Data and Spectral," no. November 2018, doi: 10.3390/rs10121862.

[9] F. Zolfaghari, V. A.-D. Management, and undefined 2022, "Determining the Most Suitable Vegetation Index for Mapping of Desertification Intensity in Arid Lands of Sistan Using Sentinel Images," *jdmal.ir,* Accessed: Feb. 14, 2023. [Online]. Available: http://www.jdmal.ir/mobile/article_251858.html?lang=en

[10] N. S. Abd-Alwahab and N. K. Ghazal, "Change Detection between Landsat 8 images and Sentinel-2 images," *Iraqi Journal of Science*, vol. 60, no. 8. pp. 1868–1876, 2019. doi: 10.24996/ijs.2019.60.8.24.

[11] Y. K. Al-timimi, L. E. George, and M. H. Al-jiboori, "Drought Risk Assessment In Iraq Using Remote Sensing And GIS Techniques," vol. 53, no. 4. pp. 1078–1082, 2012.

[12] F. A. Zwain, T. T. Al-Samarrai, and Y. I. Al-Saady, "A Study of Desertification Using Remote Sensing Techniques in Basra Governorate, South Iraq," *Iraqi J. Sci.*, vol. 62, no. 3, pp. 912–926, Mar. 2021, doi: 10.24996/IJS.2021.62.3.22.

[13] B. Abdulrahman, … K. F.-I. J. of N., and undefined 2018, "Study spectral indices of land cover around al-shari lake and produce mapping by using remote sensing technique," *researchgate.net*, 2018, Accessed: Feb. 24, 2023. [Online]. Available: https://www.researchgate.net/profile/Fouad-Mashee/publication/337682343_Study_Spectral_Indices_of_Land_Cover_Around_Al-Shari_Lake_and_Produce_Mapping_by_Using_Remote_Sensing_Technique/links/5de5659f4585159aa45ca474/Study-Spectral-Indices-of-Land-Cover-Around-Al-Shari-Lake-and-Produce-Mapping-by-Using-Remote-Sensing-Technique.pdf

[14] H. S. Abbas and A. S. Mahdi, "Study of Desertification using Remote Sensing Imagery in South

Iraq," *Journal of Science*, vol. 60, no. 4. pp. 904–913, 2019.

[15] M. F. Allawai and B. A. Ahmed, "Using Remote Sensing and GIS in Measuring Vegetation Cover Change from Satellite Imagery in Mosul City, North of Iraq," *IOP Conf. Ser. Mater. Sci. Eng.*, vol. 757, no. 1, Apr. 2020, doi: 10.1088/1757-899X/757/1/012062.

[16] I. Ibrahim, M. A.-D.-I. J. of Science, and undefined 2022, "The effect of Al-Wand lake on the shallow groundwater aquifer in Khanaqin area, Diyala Governorate, Iraq," *iasj.net*, vol. 63, no. 3, pp. 1103–1114, 2022, doi: 10.24996/ijs.2022.63.3.18.

[17] F. Mashonganyika, H. Mugiyo, E. Svotwa, and D. Kutywayo, "Mapping of Winter Wheat Using Sentinel-2 NDVI Data. A Case of Mashonaland Central Province in Zimbabwe," *Frontiers in Climate*, vol. 3. 2021. doi: 10.3389/fclim.2021.715837.

[18] E. Borgogno-Mondino, L. De Palma, and V. Novello, "Investigating Sentinel 2 Multispectral Imagery Efficiency in Describing Spectral Response of Vineyards Covered with Plastic Sheets," *Agronomy*, vol. 10, no. 12, 2020, doi: 10.3390/agronomy10121909.

[19] S. Bonafoni, M. Ieee, and A. Sekertekin, "Albedo Retrieval From Sentinel-2 by New Narrow-to-Broadband Conversion Coefficients," pp. 1–5, 2020.

[20] A. Chen, X. Yang, J. Guo, X. Xing, D. Yang, and B. Xu, "Synthesized remote sensing-based desertification index reveals ecological restoration and its driving forces in the northern sand-prevention belt of China," *Ecol. Indic.*, vol. 131, p. 108230, 2021, doi: 10.1016/j.ecolind.2021.108230.

[21] Farooq Ahmad, "Spectral vegetation indices performance evaluated for Cholistan Desert," *J. Geogr. Reg. Plan.*, vol. 5, no. 6, pp. 165–172, 2012, doi: 10.5897/jgrp11.098.

[22] "MSAVI—ArcGIS Pro | Documentation." https://pro.arcgis.com/en/pro-app/latest/arcpy/image-analyst/msavi.htm (accessed Dec. 02, 2022).

[23] H. A. A. Gaznayee *et al.*, "Drought Severity and Frequency Analysis Aided by Spectral and Meteorological Indices in the Kurdistan Region of Iraq," *Water*, vol. 14, no. 19, p. 3024, 2022, doi: 10.3390/w14193024.

[24] A. Mihi, R. Ghazela, and D. Wissal, "Mapping potential desertification-prone areas in North-Eastern Algeria using logistic regression model, GIS, and remote sensing techniques," *Environ. Earth Sci.*, vol. 81, no. 15, pp. 1–14, Aug. 2022, doi: 10.1007/S12665-022-10513-7/FIGURES/5.

[25] "TGSI: Topsoil Grain Size Index in LSRS: Land Surface Remote Sensing." https://rdrr.io/cran/LSRS/man/TGSI.html (accessed Feb. 14, 2023).

[26] N. A. T. Alani, M. M. H. Al-Shabani, and M. A. G. Al-Hiti, "Using spectral indices to assess land degradation in the Wadi al-Muhamadi basin, west of Anbar, Iraq," *Int. J. Health Sci. (Qassim).*, vol. 6, no. June, pp. 7561–7574, 2022, doi: 10.53730/ijhs.v6ns4.10916.

[27] Y. Aylin, G. Taha, H. Nikou, S. Elif, and T. Aysegul, "SENTINEL-2A IMAGES," vol. 1, no. 1, pp. 230–233, 2019.